35th Annual International Conference of the IEEE EMBS
Osaka, Japan, 3 - 7 July, 2013

The relation between temperature distribution for lung RFA and electromagnetic wave frequency dependence of electrical conductivity with changing a lung's internal air volumes

Nozomu Yamazaki, Hiroki Watanabe, XiaoWei Lu, Yosuke Isobe, Yo Kobayashi, *Member, IEEE*, Tomoyuki Miyashita, *Member, IEEE*, Masakatsu G. Fujie, *Fellow*, *IEEE*

***Abstract*— Radio frequency ablation (RFA) for lung cancer has increasingly been used over the past few years because it is a minimally invasive treatment. As a feature of RFA for lung cancer, lung contains air during operation. Air is low thermal and electrical conductivity. Therefore, RFA for this cancer has the advantage that only the cancer is coagulated, and it is difficult for operators to control the precise formation of coagulation lesion. In order to overcome this limitation, we previously proposed a model-based robotic ablation system using finite element method. Creating an accurate thermo physical model and constructing thermal control method were a challenging problem because the thermal properties of the organ are complex. In this study, we measured electromagnetic wave frequency dependence of lung's electrical conductivity that was based on lung's internal air volumes dependence with in vitro experiment. In addition, we validated the electromagnetic wave frequency dependence of lung's electrical conductivity using temperature distribution simulator. From the results of this study, it is confirmed that the electromagnetic wave frequency dependence of lung's electrical conductivity effects on heat generation of RFA.**

I. INTRODUCTION

A. Radio frequency ablation (RFA) for cancer

Radio frequency ablation (RFA) is an important modality for treating cancers and has increasingly been used over the past few years [1]-[2]. The mechanism of RF ablation shows in Figure. 1. RFA involves an electrode being percutaneously introduced into the cancer and RF energy being applied, whereupon the temperature of the tissue rises due to the ionic agitation generated by radio waves at 470 kHz. Tissue coagulation occurs as a result of protein denaturation when the tissue around the electrode reaches a temperature of around 60°C [3]. Subsequently, moisture evaporation occurs and the cancer becomes completely necrotic at 70-80°C. This percutaneous procedure, which has proven to be effective and safe, also has the advantage of being minimally invasive, meaning lower-impact operations and shorter hospital stays.

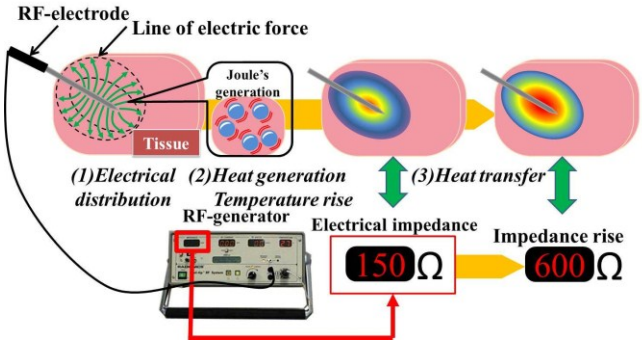

Figure. 1. Mechanism of heat transfer under RF ablation.

B. RFA for lung cancer

In recent years, the effectiveness of RFA has been reported for liver cancer and breast cancer, and as a consequence RFA is now beginning to be applied in lung cancer. The RFA procedure for lung cancer is to percutaneously puncture the cancer with the RF electrode. Subsequently using X-ray CT, the operator checks an ablation region and the relative positions of the cancer and RF electrode. Finally, the radio wave is generated on.

A characteristic of RFA for lungs is that these organs contain abundant air. Air is low in thermal conductivity and electrical conductivity. Therefore, the internal air focuses the RF energy from an electrode needle onto a limited region. Thus, the lung is more suitable for cauterization than the breast, liver or bone [1].

C. Practical shortcomings of RFA for lung cancer

However, precise cauterization of lung cancers is very difficult because the presence of pneumothorax and air inside the lung greatly affects the heat transfer and temperature distribution near a RF electrode. In fact, excessive ablation or non-ablation of cancers has been reported in lung RFA treatment [4]. In the case of the lung as compared with other organs such as the liver, the actual ablation lesion may not coincide with the original region that was targeted by the operator. Additionally, although the temperature distribution

Manuscript received January 18, 2013. This work was supported in part by the Global COE (Centers of Excellence) Program "Global Robot Academia", in part by a Grant for Scientific Research 22360108.

N. Yamazaki, H. Watanabe, X. W. Lu, Members of Graduate Schools of Advanced Science and Engineering, Waseda University, Japan. (59-309, 3-4-1, Okubo, Shinjuku Ward, Tokyo, Japan. E-mail: nozomu0626@akane.waseda.jp; Tel: +81-3-5286-3412; Fax: +81-3-5291-8269).

Y. Isobe, Member of Graduate Schools of Creative Science and Engineering, Waseda University, Japan.

Y. Kobayashi, T. Miyashita and M. G. Fujie, Members of the Faculty of Science and Engineering, are with the Graduate School of Science and Engineering, Waseda University, Japan.

of the ablation region is invisible, it is possible using RFA in combination with X-ray CT to determine protein denaturation during cautery for lung cancers. So, the pattern of heat transfer during lung RFA and increase in tissue temperature near the RF needle is not clear.

II. Objectives

The objective of this study has being to develop a model-based robotic ablation system for the support of RFA treatment of lung cancer, using a computer simulator based on an accurate thermal physical model of a lung. The proposed robotic surgical system attempts to provide a creating coagulation lesion by accurate heating to a cancer and visual information on the condition of the cauterized cancer for the operator. It involves:

1) Optimized RF energy to cauterize the lung cancer
2) Appreciation of the ablation legion and ablation time
3) Heat transfer to the normal tissue adjacent to the cancer

In order to achieve our objective, the purpose of this paper is that the relation between temperature distribution for lung RFA and electromagnetic wave frequency dependence of electrical conductivity with changing a lung's internal air volumes. Because the size of ablation lesion greatly affected by heat generation from RF electrode. This heat generation is determined by electrical conductivity. Electrical conductivity has properties which is electromagnetic wave frequency dependence. Thus, it is supposed that if it control electromagnetic wave frequency variably, it is possible that a heat generation value and a size of ablation lesion are able to control. However, it is not clear that how the lung's electrical conductivity depend on electromagnetic wave frequency. Additionally, it confirmed from our previous study that the lung's electrical conductivity is changed with lung's internal air volumes [5]. Therefore, the novelty work of the presence study is in measuring electromagnetic wave frequency dependence of electrical conductivity with changing a lung's internal air volumes, and in validating this dependence by using temperature distribution simulator.

This report is organized as follows: Section III describes the method of measuring electromagnetic wave frequency dependence of electrical conductivity with changing a lung's internal air volumes, and validating the dependence by using temperature distribution simulation with measurement values. In Section IV and V the results and discussion are presented. Finally, Section VI details our conclusions and plans for future work.

III. Materials and Methods

A. In vitro experiment

1) Lung's internal air pressure control method

In order to measure electrical conductivity when air is contained in the lung, we developed a pressure control unit. The overview of controlling swine lung's internal air pressure by the unit are shown in figure 2.The air, which was compressed by a compressor, is supplied to the lung by means of a pressure regulation valve, a flow-regulating valve, a solenoid valve, a rumen tube and an air hose. The pressure control machine is able to supply air to the lung with a flow rate of 3.0 L/min. This flow rate is the same as the flow rate of air during human breath motion. Lung internal pressure is enable to be controlled to become higher than atmospheric pressure using the pressure control machine. It is possible to expand hog lung using this machine to a pressure of 3.0 kPa over atmospheric pressure.

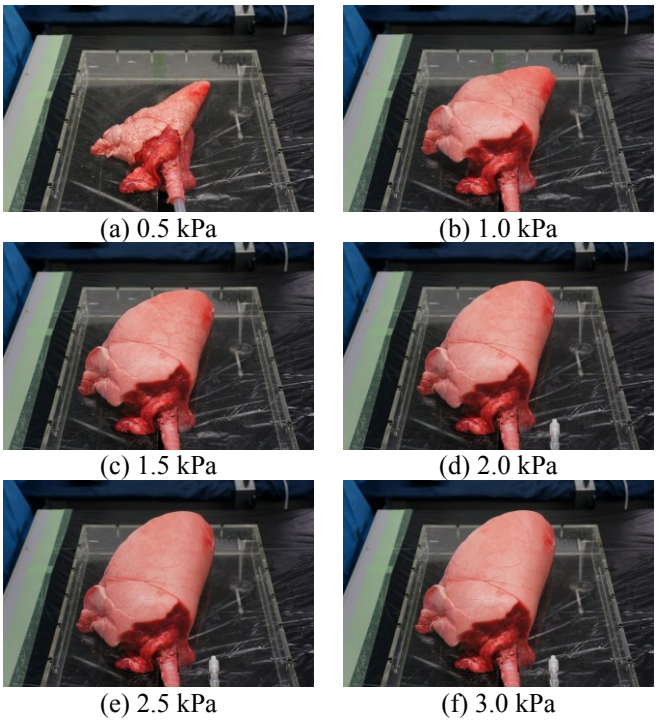

(a) 0.5 kPa (b) 1.0 kPa (c) 1.5 kPa (d) 2.0 kPa (e) 2.5 kPa (f) 3.0 kPa

Figure. 2. A swine lung size of each a swine lung's internal air pressure.

2) Measurement of lung's electrical conductivity

In order to measure the electromagnetic wave frequency dependence of lung's electrical conductivity with changing a lung's internal air volumes, we chose Four Electrodes Method with Alternating current to measure electromagnetic wave dependence. The four electrode probes with a low impedance metal were inserted into an aerated swine lung. Each low impedance metal probe was arranged at 10 mm intervals. The length of the four probes was 10 mm and the diameter was 1.0 mm. They were inserted into 10 mm depth from an aerated lung surface. To measure the electrical conductivity of a lung parenchyma, we chose and the probes inserted into a distal portion of lung. As presented above, we measured the electrical conductivity at 0.5 kPa intervals from 0.5 to 3.0 kPa using a Impedance analyzer (Chemical Impedance Meter, 3532-80 Hioki E.E. Corporation, Nagano, Japan) with changing input frequency from 4 Hz to 470 kHz.

The overview of experimental set up and measuring electrical conductivity are shown in Figure. 3 and 4. The array of low impedance metal is shows in Figure. 5.

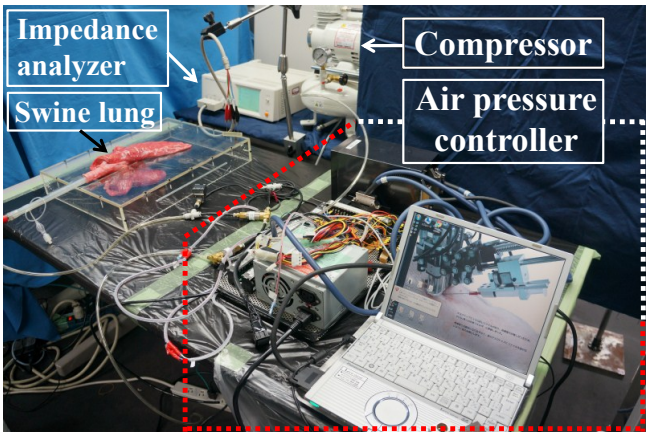

Figure. 3. Overview of Experimental set up.

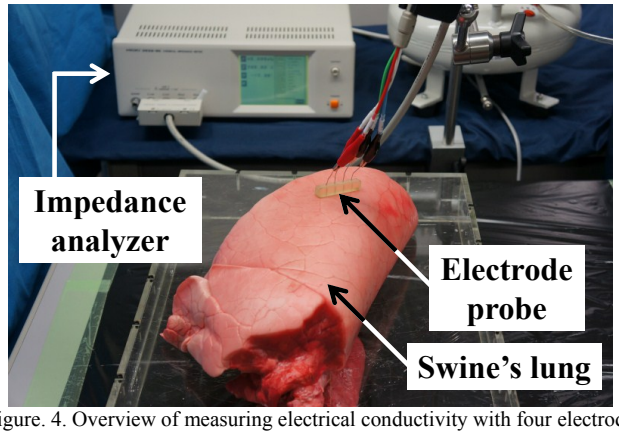

Figure. 4. Overview of measuring electrical conductivity with four electrode probe at 3.0kPa.

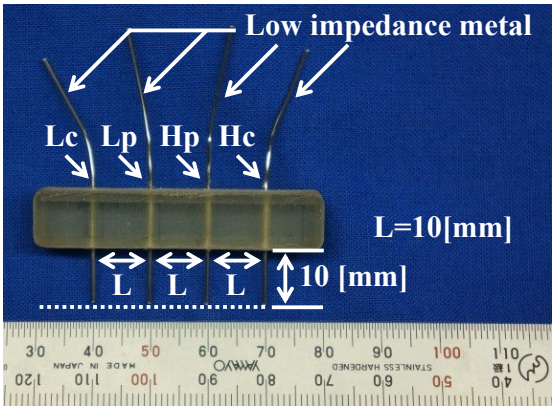

Figure. 5. The array of low impedance metal probe.

Principal: The principle of Four Electrodes Method with Alternating current is shown in figure 6. First of all, four electrode probes insert into samples. Secondly, Alternating current power unit generate alternating current to the samples. Finally, the unit measure impedance and calculate electrical conductivity. Calculus equation of electrical conductivity is shown in equation (1) ~ (3). Where σ is the electrical conductivity of samples [S/m], ρ its electrical resistivity of samples, R its impedance of samples [Ω･m], L its the probe distance between Hp and Lp[m], and S the cross-sectional area of current transfer. In this experiment, we set L = 10 mm and S = 78.5 mm^2.

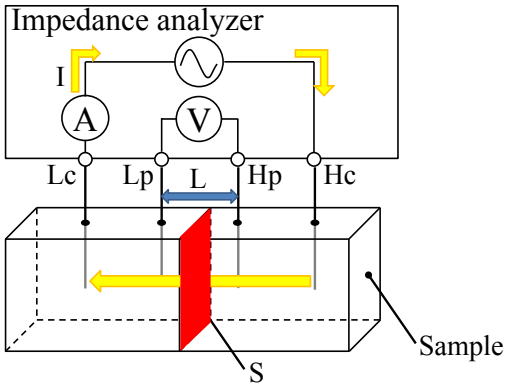

Figure. 6. Four Electrodes Method with Alternating current.

$$\sigma = \frac{1}{\rho} \tag{1}$$

$$R = \frac{\rho L}{S} \tag{2}$$

$$\sigma = \frac{L}{RS} \tag{3}$$

3) Results

Figure 7 shows the result of electromagnetic wave frequency dependence of lung's electrical conductivity with changing lung's internal air pressure with five individuals. The result plots are average value of five individuals. The value of aerated lung's electrical conductivity at 1.5 kPa and at 470 kHz was 0.174 [S/m] which is the least value in measurement points. According to the results of our study, three tendencies were provided. Domain A, lung's internal pressure is from 0.5 kPa to 1.5 kPa and frequency is from 40 kHz to 470 kHz, decrease a value of electrical conductivity with increasing frequency. And, domain B is lung's internal pressure is from 1.5 kPa to 3.0 kPa and frequency is from 40 kHz to 470 kHz. In domain B, lung's electrical conductivity decrease with increasing frequency until 470 kHz. Domain C is lung's internal pressure is from 0.5 kPa to 3.0 kPa and frequency is from 4Hz to 40 kHz. In domain C, lung's electrical conductivity increase with increasing frequency until 40 kHz.

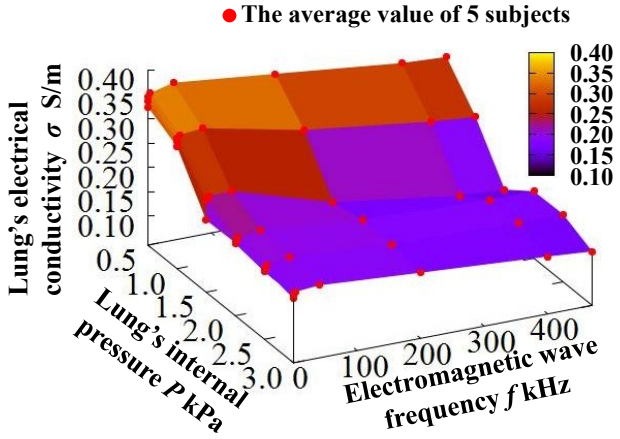

Figure. 7. Pressure dependence of lung's electrical conductivity from 4Hz to 470kHz.

B. Simulation

1) Thermophysical model of organs

In order to construct model-based robotic ablation system, we modeled lung's thermal properties and electrical properties for heat transfer during RFA. The thermal and electrical properties are included in the bio heat equation (4) that is required to calculate the tissue temperature around a cancer [6]-[7].

$$\rho C \frac{\partial T}{\partial t} = \lambda \nabla^2 T + \sigma |E|^2 - \rho \rho_c C_b F (T - T_b) + Q_m \qquad (4)$$

where ρ is the density of the organ [kg/m^3], c its specific heat [J/kgK], T its temperature in °C, λ its thermal conductivity [W/mK], σ its electrical conductivity [S/m], E its electrical field [V/m], ρ_b the density of blood, c_b the heat capacity of blood, F the blood perfusion coefficient of the organ [m^3/kgs], θ_b the blood temperature and Q_m the metabolic heat source term of the organ [W/m^3]. The left-hand clause 1 is heat capacity. The right-hand clause 1 is heat transfer. Clause 2 is the heat value from the RF electrode and clause 3 is the absorption of heat by organ's blood flow.

In this study, we measured lung's electrical conductivity in vitro condition. Therefore, we operated temperature distribution simulation by using the heat equation (5). This equation is deleted the absorption of heat by organ's blood flow and metabolic heat source term.

$$\rho C \frac{\partial T}{\partial t} = \lambda \nabla^2 T + \sigma |E|^2 \qquad (5)$$

2) Temperature distribution simulator

We constructed a temperature distribution simulator for lung RFA (Fig. 8). The finite element method (FEM) simulator consisted of 4235 elements and 22152 nodes. Figure 8a shows the lung simulator before RFA. Figure 8b shows the temperature rise near a RF electrode at 600 s after RFA. The constructed simulator was validated using an in vitro experiment, and the lung's internal heat transfer was validated quantitatively from the viewpoint of the RFA heat transfer mechanism.

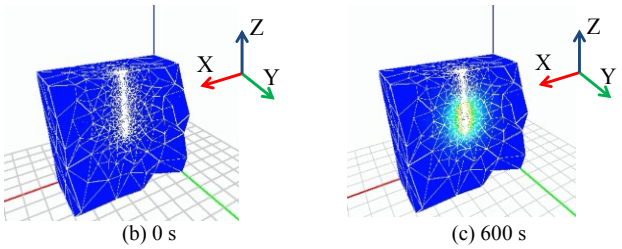

(b) 0 s (c) 600 s

Figure. 8. Temperature distribution simulator for lung RFA [6]-[7].

Figure 9 shows the parameter of lung's thermal and electric properties used for the simulation. The model was 70 mm in length, 70 mm in width and 50 mm in depth. The RF electrode was inserted from the X-Y plain surface to a depth of 35 mm towards the Z-axis. In order to determine the heat value from the RF electrode, it was necessary for the electrical field distribution to be close to the needle. The RF electrode that was used in the in vitro study generated radio waves from near the needle tip to the tip. The distance was 20 mm. Therefore, electrical field analysis was input at 60 V in part of the needle tip and 0 V in the return electrode on the X-Y plain. In other boundaries the insulation condition due to surface contact with air or needle insertion was determined. After the specific heat value was determined, temperature distribution was calculated from thermal analysis using equation (5). It was used to set two types of thermal analysis boundary conditions. One was the heat transfer condition between the needle surface and lung tissue. The other was the heat insulation condition, and the boundary was the same as that of the lung surface that was in contact with air. The reason for the heat insulation condition was that air has a very low thermal conductivity, and a value that is much lower than the organ's thermal conductivity. Thus, it sets the heat insulation condition on the lung surface. The boundary temperature was 20°C where is experimental room air temperature.

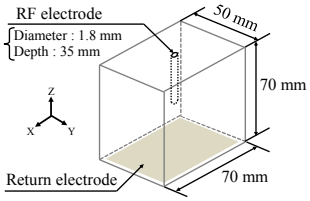

Figure. 9. Shape model of temperature distribution simulation [7].

Under the above-mentioned simulation conditions temperature distribution during RFA was calculated by input of the organ's thermal and electrical parameters. From the result of measuring electromagnetic frequency dependence of electrical conductivity, we set four pattern analyses.

Firstly, the specific heat value was 2500 [J/kgK] in all of the four pattern analyses, because the specific heat does not change the lung's internal air as has been previously reported [8]. Secondly, the four pattern analyses were set at 60 V input. The three lung properties of thermal conductivity, electrical conductivity and density were changed by variations in the lung's internal air volume. In addition, electrical conductivity is changed by using electromagnetic frequency. The simulation used measured values of thermal and electrical conductivity and density values published in the literature [7]-[8]. Lung's thermal conductivity and density calculated from equation (6), (7) and (8) by input lung's internal air pressure.

The measured and calculated thermal and electrical properties are shown in Table I and Table II. The parameter pattern A used the measurement point parameter which is at P = 1.5kPa and f = 470 kHz in figure. 7. Other three patterns are the points where large deference of electrical conductivity value compared with at P = 1.5kPa and f = 470 kHz.

$$\lambda = -0.013P + 0.157 (P > 0.5kPa) \qquad (6)$$

$$\lambda = 0.203 \cdot e^{-0.60 \cdot P} (P < 0.5kPa) \qquad (7)$$

$$\rho = -80P + 480 (0 \le P \le 3.0kPa) \qquad (8)$$

TABLE I
Input parameter patterns of lung's internal pressure and electromagnetic wave frequency for the temperature distribution simulator

Parameter Pattern	*Lung's internal pressure P kPa*	*Electromagnetic wave frequency f kHz*
A	0.5	470
B	1.5	40
C	1.5	470
D	3.0	470

TABLE II
Input parameters for the temperature distribution simulator by calculations value from measurement value

Parameter pattern	*Thermal Conductivity W/mK*	*Electrical Conductivity S/m*	*Density kg/m^3*
A	0.150	0.309	280
B	0.138	0.264	320
C	0.138	0.174	480
D	0.125	0.151	240

IV. Results

The results of temperature distribution analysis up to 200 sec are shown in Figure 10. When we cauterized collapsed swine lungs at 0 kPa, the RF generator became Roll-off within 120 sec [7]. This time was shorter than cases of aerated lungs. So, we analyzed temperature distribution until 200 sec.

In parameter pattern A ~ D, tendency of temperature rise at 10 and 15 [mm] from RF electrode tip was not difference. The tendency of temperature at 10 and 15 mm was rising with increasing ablation time. But, these tendency of temperature rising were slowly increasing which were compared with temperature rising at 5 [mm]. However, the nearest temperature simulation point at 5 [mm] is large difference after 200 sec from ablation simulation start. In 200 sec after ablation start, temperatures are arranged in order of Parameter pattern A, B, C, D at 5 [mm]. Parameter pattern A was the highest temperature at 5 [mm] after 200 sec in all four analyses pattern. In particular, parameter pattern C was similar to parameter pattern D. The deference of two analyses was lung's internal pressure.

V. Discussion

1) Electromagnetic dependence of electrical conductivity

In this paper, we have presented data concerning the electromagnetic wave frequency dependence of lung's electrical conductivity with changing a lung's internal air volumes. From the experiments it was suggested that the frequency dependence of changing a lung's internal air volumes had an effect on heat transfer.

Domain A is suggested that decreasing of electrical conductivity is more affected by insulation effect with increasing lung's internal air volumes than electromagnetic frequency dependence. On the other hand, domain B is suggested that increasing of electrical conductivity more than

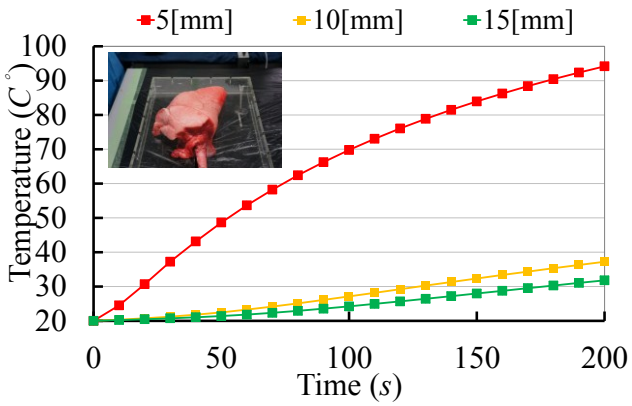

(a) Parameter pattern A

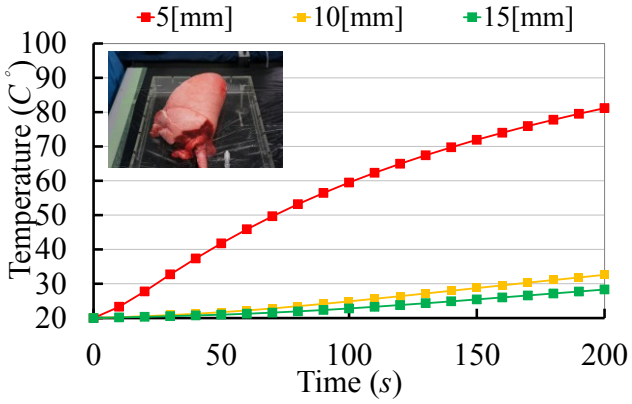

(b) Parameter pattern B

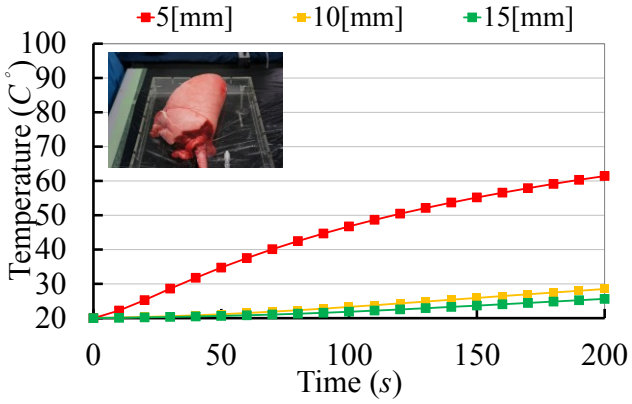

(c) Parameter pattern C

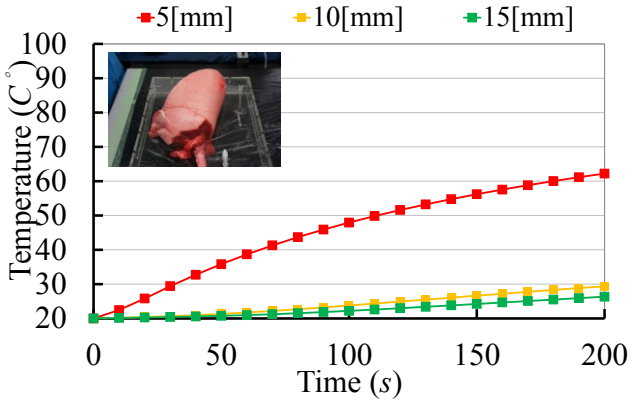

(d) Parameter pattern D

Figure. 10. Results from temperature distribution simulation.

470 kHz is more affected by electromagnetic frequency dependence than insulation effect with increasing lung's internal air volumes. It is supposed that these differences are caused by changing ratio of a lung parenchyma and lung's internal air volumes. Thus, if it input high electromagnetic frequency into lung tissue which contained abundant air, it is possible that ablation lesion is larger than using radiowaves at 470 kHz.

2) Temperature distribution

Electrical conductivity is decreasing with electromagnetic wave frequency increasing from 40 kHz to 470 kHz. A swine lung from 0.5 kPa ~ 3.0 kPa, a value of electrical conductivity is the highest at 40 kHz. Therefore, electromagnetic wave at 40kHz is easy to electrical current and the heat generation from RF electrode is large other frequency within 470kHz. It is suggested that 40 kHz is the most suitable for ablation for a lung under 470 kHz.

In addition, it was confirm that ablation lesion area is change, in spite of the same temperature rising tendency in parameter pattern C and D. Even if temperature rising tendency is the same, size of lung is difference because of lung's internal air pressure difference between parameter pattern C and D. In the case of pattern C and D, it is supposed that ablation lesion of parameter pattern C is more large than parameter pattern D because density of parameter pattern C is larger than pattern D. Thus, lung tissue at 1.5kPa is dense than at 3.0kPa and it is possible that it is able to cauterize lung tissue at 1.5kPa than at 3.0kPa under the same frequency.

From the view point of thermal distribution control by robotics approach, it is effective that electromagnetic wave frequency change correspond with lung's internal air volumes during ablation therapy. Because heat generation from RF electrode is able to control not changing input voltage but changing electrical impedance by controlling electromagnetic frequency during therapy. However, published in the literature described that electrical conductivity of microwave at 2.45 GHz is higher than that of radiowave at 470 kHz [1]. So, a heat generation of microwave is larger than radiowave. From this point, ablation using microwave is effective of large size of a lung cancer. On the other hand, microwave ablation is not effective comparison with RFA. Because microwave ablation has large heat generation, so it is able to cauterize large size of a cancer, but it would be cauterized excessive near RF electrode tissue. If it control heat generation and temperature distribution near RF electrode, radiowave is possible that precise and adapt thermal dose control by robotic ablation system. Because, even if lung's internal air volumes and using electromagnetic wave frequency for ablation are change, the variation value of electrical conductivity is small.

In this study, it is suggested that ablation for a lung using electromagnetic wave frequency less than radiowave at 470 kHz is effective to use control thermal dose and temperature near RF electrode due to precise and adapt control using robotic ablation system. Changing electromagnetic wave frequency is effective for precise ablation lesion control.

VI. Conclusions and Future work

In this paper, we presented the relation between temperature distribution for lung RFA and electromagnetic wave frequency dependence of electrical conductivity with changing a lung's internal air volumes. From the experiments it was suggested that the frequency dependence of changing a lung's internal air volumes had an effect on heat transfer. And, From the view point of thermal distribution control by robotics approach, it is effective that electromagnetic wave frequency change correspond with lung's internal air volumes during ablation therapy. In particular, it uses less than 470 kHz. Low electromagnetic wave frequency ablation is able to precise and adapt thermal control correspond with lung's internal air volumes.

In the future, more detailed validations of the air volume of thermal and electric physical properties on lung internal air volumes will be necessary. Firstly, we will have to decide suitable electromagnetic wave frequency and develop to control method of electromagnetic wave frequency for a lung cancer ablation. Additionally, we will further develop a thermal control system during RFA for safe and precise clinical RFA treatment of lung cancers.

References

[1] S. N. Goldberg, "Radiofrequency tumor ablation: principles and techniques," European Journal of Ultrasound, vol.13, pp. 129-147, 2001

[2] T. Hiraki, H. Gobara, H. Mimura, Y. Sano, T. Tsuda, T. Iguchi, H. Fujiwara, R. Kishi, Y. Matsui, S. Kanazawa, "Does tumor type affect local control by radiofrequency ablation in the lungs?," European Journal of Radiology, vol.74, pp. 136-141, 2010

[3] XiaoWei Lu, Mariko Tsukune, Hiroki Watanabe, Nozomu Yamazaki, Yosuke Isobe, Yo Kobayashi, Tomoyuki Miyashita, and Masakatsu G. Fujie, "A Method for Deriving the Coagulation Boundary of Liver Tissue Using a Relational Model of Viscoelasticity and Temperature in Radio Frequency Ablation", Proceeding of 34rd Annual International Conference of the IEEE Engineering in Medicine and Biology Society, pp. 187-190, 2012

[4] A. Pennathur, G. Abbas, R. J. Landreneau, J. D. Luketich, "Radiofrequency Ablation for the Treatment of Stage 1 Non- Small Cell Lung Neoplasm," Semin Thorac Cardiovasc Surg, vol.20, pp.279-284, 2008

[5] N.Yamazaki, Y. Isobe, H. Watanabe, T. Hoshi, Y. Kobayashi, T. Miyashita, M. G. Fujie, "Modeling the dependence of electrical conductivity on internal lung pressure for lung RFA", Computer Assisted Radiology and Surgery 26th International Congress and Exhibition, S198-S199, 2012

[6] H. Watanabe, N. Yamazaki, Y. Kobayashi, T. Miyashita, T. Ohdaira, M. Hashizume, M. G. Fujie, "Estimation of Intraoperative Blood Flow during Liver RF Ablation Using a Finite Element Method-based Biomechanical Simulation," Proceeding of 33rd Annual International Conference of the IEEE Engineering in Medicine and Biology Society, pp. 7441-7446, 2011

[7] Nozomu Yamazaki, Hiroki Watanabe, XiaoWei Lu, Yosuke Isobe, Yo Kobayashi, Tomoyuki Miyashita, Masakatsu G. Fujie, "Development of a temperature distribution simulator for lung RFA based on air dependence of thermal and electrical properties", Proceeding of 34rd Annual International Conference of the IEEE Engineering in Medicine and Biology Society, pp. 5699-5702, 2012

[8] H. Futami, T. Arai, H. Yashiro, S. Nakatsuka, S. Kuribayashi, Y. Izumi, N. Tsukada, M. Kawamura, "A Heat Conduction Simulator to Estimate Lung Temperature Distribution During Percutaneous Transthoracic Cryoablation for Lung Cancer," JSMBE, vol. 44, num 3, pp. 460-466, 2008